



IJRASET

International Journal For Research in
Applied Science and Engineering Technology



INTERNATIONAL JOURNAL FOR RESEARCH

IN APPLIED SCIENCE & ENGINEERING TECHNOLOGY

Volume: 14 **Issue:** V **Month of publication:** May 2026

DOI: <https://doi.org/10.22214/ijraset.2026.83292>

www.ijraset.com

Call:  08813907089

E-mail ID: ijraset@gmail.com

Influence of Variable Viscosity on Hydrodynamic and Thermal Characteristics of Casson Fluid Flow over a Stretching Surface

Bhanoth Rajender

Department of Mathematics, Anurag University, Hyderabad, TS, India - 500088

Abstract: *This research examines the steady two-dimensional boundary-layer flow and thermal behavior of a Casson fluid over a stretching surface, taking into account viscosity variations with temperature. Using suitable similarity transformations, the governing momentum and energy equations are transformed into ordinary differential equations. These equations are then solved numerically using the successive linearisation method. Special attention is given to the effects of the Casson parameter, variable viscosity, and the Prandtl number on the velocity and temperature distributions. The results reveal that stronger non-Newtonian effects tend to slow down the fluid motion and thicken the momentum boundary layer, while higher Prandtl numbers lead to a reduction in the thermal boundary-layer thickness. Viscosity variation is also found to significantly influence both the hydrodynamic and thermal behavior of the fluid. These findings contribute to a better understanding of transport phenomena in non-Newtonian fluid flows over stretching surfaces and are relevant to various engineering and industrial processes.*

Keywords: *Casson fluid, stretching sheet, variable viscosity, heat transfer.*

I. INTRODUCTION

Research involving flow over a radially stretching sheet has attracted considerable attention because of its wide relevance in Chemical Engineering, Metallurgy, and Biomedical Engineering, as well as in applications such as paper manufacturing, polymer processing, molten metal treatment, and glass fiber production. Owing to these practical applications, numerous studies have investigated heat and mass transfer behavior in both Newtonian and non-Newtonian fluid flows, with emphasis on understanding their thermal and flow characteristics under various physical conditions. Khan et al. [1] analyzed the axisymmetric flow behavior and thermal transport of a Cross fluid induced by a radially stretching surface. The study emphasized how the stretching motion influences transport processes and boundary-layer development, thereby affecting both momentum and thermal distributions. Ahmed et al. [2] examined the combined influence of a tilted magnetic field and radiative heat transfer on the behavior of a Sisko fluid flowing over a surface that stretches radially. The study demonstrates how these factors modify velocity distribution, heat transfer behavior, and the development of momentum and thermal boundary layers. Sreelakshmi et al. [3] assessed the Jeffrey nanofluid's time-dependent flow dynamics and temperature characteristics on a radially stretching surface while taking convective boundary effects into account. The homotopy analysis method was used to solve the problem, enabling an examination of how time-dependent effects and fluid parameters influence velocity, temperature distribution, and nanoparticle concentration profiles. Khan et al. [4] examined how various slip conditions influence axisymmetric magnetohydrodynamic buoyancy-driven nanofluid flow over a stretching surface, with particular emphasis on the impacts of thermal radiation and chemical reaction processes in modifying velocity profiles, temperature distribution, concentration fields, and overall transport behavior within the fluid system. Nayak et al. [5] examined the impact of a chemical reaction on mass transfer in a flow across a sheet that is stretching radially, showing that reactive effects significantly modify concentration transport and boundary-layer behavior. Unlike many earlier investigations focused on steady-state conditions, this study also emphasized unsteady flow characteristics, demonstrating the importance of time-dependent behavior in engineering transport processes. Shahzad et al. [6] investigated transient Heat transfer and axisymmetric flow on a radially extending surface with time-dependent characteristics. The analysis highlights the significance of unsteady effects in influencing transport processes, including variations in velocity and temperature distributions within the boundary layer. The study also highlighted the importance of analyzing Non-Newtonian fluid behavior in industrial applications, noting that unlike simple Newtonian fluids, complex fluids exhibit diverse rheological properties that cannot be fully represented by a single universal constitutive model. Nadeem et al. [7] examined the flow behavior of a Casson fluid over a porous linearly stretching sheet, showing how a transverse magnetic field influences fluid motion, boundary-layer development, and associated transport characteristics.

Mahanta and Shaw [8] analyzed the flow dynamics and heat transfer performance of a Casson fluid over a permeable sheet stretching linearly, subject to convective boundary conditions, and demonstrates how permeability and thermal convection affect boundary-layer structure and transport mechanisms. Raju [9] investigated heat and mass transport in Magnetohydrodynamics propagation of a Casson fluid over a porous surface that is exponentially stretching, demonstrating the effects of magnetic forces and permeability on thermal behavior, concentration distribution, and boundary-layer transport. Malik et al. [10] investigated the flow behavior of a Casson fluid over a stretching surface in the presence of variable viscosity, non-uniform thickness, and an external magnetic field while employing the Cattaneo–Christov heat flux formulation to evaluate their influence on momentum and heat transfer characteristics. Nawaz et al. [11] investigated the consequences of varying thermal conductivity, Joule heating, and viscous dissipation on a Casson fluid's flow along a stretched surface, highlighting their strong impact on temperature distribution, fluid dynamics, and overall transport behavior. Awais et al. [12] examined the thermal and concentration transport behavior of a Casson fluid flowing through a porous medium over a shrinking surface, accounting for internal heat source or sink effects along with an applied transverse magnetic field. The results reveal how these parameters modify boundary-layer formation and influence temperature and concentration distributions within the flow. Sohail et al. [13] investigated This study investigates entropy generation in Casson fluid flow over a nonlinear bidirectionally stretching surface, incorporating the effects of variable thermal conductivity and heat transfer properties. The analysis highlights how these factors influence irreversibility and thermal performance within the flow system and demonstrated their influence on irreversibility and transport behavior. The study also emphasized the industrial significance of radially stretching surfaces while noting the comparatively limited research available for Casson fluid flow in such configurations. Faraz et al. [14] examined axisymmetric Casson fluid flow over an unsteady radially stretching sheet, highlighting the combined effects of Soret effect, multiple slip conditions, chemical reaction, and magnetic forces on transport behavior. The study further showed that simultaneous heat and mass transfer leads to complex coupling between temperature and concentration gradients, significantly influencing energy and species transport mechanisms. Hayat et al. [15] investigated the characteristics of MHD Casson fluid flow over a stretching sheet under the influence of Soret and Dufour effects, highlighting their significant role in coupling heat and mass transfer processes and shaping the overall transport behavior. Kameswaran et al. [16] examined the behavior of a Casson fluid near the stagnation region over a stretching surface, emphasizing its effect on boundary-layer formation and overall transport processes. Sharada [17] analyzed mixed convection magnetohydrodynamic flow of a Casson fluid over a surface undergoing exponential stretching, taking into account the combined effects of Soret and Dufour diffusion, chemical reactions, and thermal radiation. The findings illustrate how these factors influence velocity profiles, heat transfer rates, and mass transport within the boundary layer. Oyelakin et al. [18] examined the flow of a Casson nanofluid over an unsteady stretching sheet, focusing on the roles of Soret and Dufour effects, while also accounting for thermal radiation and internal heat generation, highlighting their influence on velocity distribution, temperature field, and coupled mass transfer mechanisms within the boundary layer. Vinod Y et al. [19] analyzed the heat transfer characteristics and magnetohydrodynamic boundary-layer behavior of a non-Newtonian Casson fluid over a surface undergoing exponential stretching. The study further considers the effects of thermal radiation along with internal heat generation or absorption. Sarma Ak et al. [20] examined the unsteady, two dimensional free convective Darcy Forchheimer Casson fluid flow under magnetohydrodynamic (MHD) effects over a vertically stretching sheet, taking into account the influence of gyrotactic microorganisms as a key feature of the analysis. Subhashini et al. [21] examined the coupled influence of thermal and mass Biot numbers on the behavior of two-dimensional steady incompressible viscous Powell Eyring model flow, and found that variations in these parameters significantly modify velocity, temperature, and concentration distributions, with corresponding changes in heat and mass transfer characteristics. Triveni B et al. [22] examined the combined roles of chemical reaction, spatially varying heat source, viscous dissipation, Brownian diffusion, and thermophoresis in MHD Casson nanofluid flow, revealing notable changes in transport characteristics and boundary layer behavior over the nonlinear stretching sheet. MinZ et al. [23] examined magnetohydrodynamic (MHD) flow and bioconvection in nanofluids for their important contribution to improving heat transfer characteristics. In hydrogen energy technologies, particularly fuel cells, efficient thermal management is essential because it strongly impacts system performance, stability, and long-term durability. Upreti H et al. [24] examined the combined flow dynamics and thermal efficiency of a water-based hybrid nanofluid with single-walled and multi-walled carbon nanotubes over a stretching sheet, with emphasis on how these components affect heat transfer and fluid motion within the boundary layer. Awati VB et al. [25] explored magnetohydrodynamic Studied heat and mass transfer behavior in an upper-convected Maxwell nanofluid flowing over a porous stretching surface under the influence of gyrotactic microorganisms. Both numerical and semi-analytical approaches are employed to examine the resulting flow, thermal, and concentration characteristics.

II. MODEL FORMULATION AND GEOMETRICAL SETUP

An incompressible Casson fluid's ongoing, two-dimensional laminar boundary-layer flow is measured across a stretching sheet situated at $y = 0$. The sheet swings with a velocity in the x -direction defined as $U_w(x) = ax$ where $a > 0$ represents a constant rate of stretching. The fluid domain is limited to the area $y > 0$. The x -axis is placed down the sheet using a Cartesian coordinate system, while the y -axis is perpendicular to it. The corresponding velocity components are denoted by $u^3(x, y)$ in the x -direction and $v^c(x, y)$ in the y -direction. The temperatures of the sheet and the ambient fluid are given by $T_w(x), T_\infty$ respectively. It is expected that the fluid's dynamic viscosity fluctuates with temperature and is expressed as $\mu = \mu(T)$. The flow is induced purely by the stretching action of the surface. Under the boundary-layer assumptions, the velocity gradients in the direction normal to the sheet are considered significantly larger than those along the sheet.

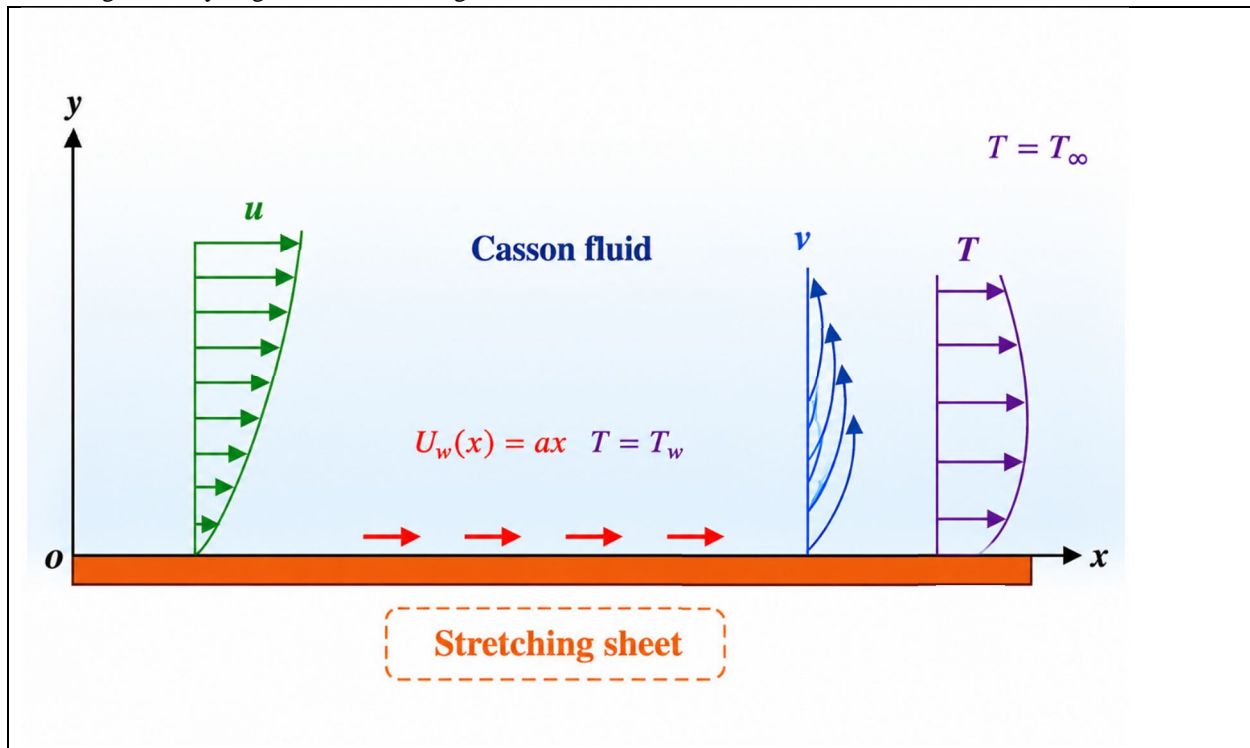


Figure 1. Flow domain structure

III. GOVERNING MATHEMATICAL FRAMEWORK

To reflect the consequences of temperature on fluid properties, the kinematic viscosity is represented as $\nu(T) = \left(\frac{1}{1 + \xi(T - T_\infty)}\right) \nu_0$ where ξ has a viscosity of variation parameter. Based regarding the boundary-layer theory, the equations governing mass, The following is how momentum and energy conservation are defined and expressed

$$\frac{\partial^k u}{\partial x} + \frac{\partial^k v}{\partial y} = 0 \tag{1}$$

$$u \frac{\partial^i u}{\partial x} + v \frac{\partial^i u}{\partial y} = \left(1 + \frac{1}{\beta}\right) \left(\nu(T) \frac{\partial^2 u}{\partial y^2} + \frac{d\nu(T)}{dT} \frac{\partial T}{\partial y} \frac{\partial u}{\partial y} \right) \tag{2}$$

$$u^d \frac{\partial T}{\partial x} + v^d \frac{\partial T}{\partial y} - \alpha^d \frac{\partial^2 T}{\partial y^2} = 0 \tag{3}$$

$$\left. \begin{aligned} u = U_w(x) = ax, \quad v = 0, \quad T = T_w \quad \text{at } y = 0 \\ u \rightarrow 0, \quad T \rightarrow T_\infty \quad \text{as } y \rightarrow \infty \end{aligned} \right\} \tag{4}$$

Similarity variables are introduced following the standard stretching sheet transformation:

$$\eta^d = \left(\frac{a}{\nu_0}\right)^{\frac{1}{2}} y, \quad u^g = axf'(\eta), \quad v^g = -(\alpha\nu_0)^{\frac{1}{2}} f(\eta), \quad \theta^d(\eta)(T_w - T_\infty) + T_\infty = T^d \tag{5}$$

$$v^* = (1 + \xi^* \theta)^{(-1)}$$

Substituting these expressions into Eqs. (2)– (3) yields

$$\left(1 + \frac{1}{\beta}\right) (v^* f''' + (v^*)' f'') + f f'' - (f')^2 = 0 \tag{6}$$

$$\theta'' + Pr f \theta' = 0 \tag{7}$$

The corresponding Boundary conditions are constraints applied at the boundaries of a problem:

$$\left. \begin{aligned} \eta = 0: f^*(0) = 0, f'(0) = 0, \theta(0) = 1 \\ \eta \rightarrow \infty: f^{*'}(\infty) = 0, \theta(\infty) = 0 \end{aligned} \right\} \tag{8}$$

Critical engineering quantities are the wall shear stress, typically characterized by the skin-friction coefficient at a point and the corresponding Nusselt number which quantifies the surface warmth transfer rate. The skin-friction coefficient throughout its nondimensional form is given by (C_f) and the Nusselt factor (Nu) are

$$C_f^* = f''(0) \text{ and } Nu^* = -\theta'(0)$$

IV. METHOD OF SOLUTION

The described nonlinear boundary value distribute by Eqs. (6) – (8) is addressed numerically implementing the method of successive linear treatment (SLM). The resulting linear subproblems are then solved through the Chebyshev collocation technique. Within the SLM framework, the unknown functions are initially assumed in an iterative form.

$F(\eta) = [f(\eta), \theta(\eta)]$ can be taken as

$$F(\eta) = F_j(\eta) + \sum_{m=0}^{i-1} F_m(\eta), \tag{9}$$

Here, $F_j(\eta)$ ($j = 1, 2, \dots$) denote the unknown functions, while $F_m(\eta)$ represents an approximate solution. This approximation is obtained by solving the linearized system of equations formed by substituting. By inserting Eq. (8) into Eqs. (6) – (7) and omitting the nonlinear terms associated with f_j and θ_j the resulting set of linear equations can be written as follows

$$a_1 f_j''' + a_2 f_j'' + a_3 f_j = r_1 \tag{10}$$

$$b_1 f_j + b_2 \theta_j'' + b_3 \theta_j' = r_2 \tag{11}$$

where

$$a_1^* = 2\eta[1 + 1/\beta],$$

$$a_2 = 2\eta[1 + 1/\beta] + \sum_{m=0}^{j-1} f_m$$

$$a_3 = \sum_{m=0}^{j-1} f_m''$$

$$r_1 = -2\eta[1 + 1/\beta] \sum_{m=0}^{j-1} f_m''' - 2[1 + 1/\beta] \sum_{m=0}^{j-1} f_m'' - \sum_{m=0}^{i-1} f_m \sum_{m=0}^{j-1} f_m''$$

$$b_1 = Pr/2 \sum_{m=0}^{j-1} \theta_m',$$

$$b_2 = \eta, \quad b_3 = 1 + Pr/2 \sum_{m=0}^{j-1} f_m,$$

$$r_2 = -Pr/2 \sum_{m=0}^{j-1} f_m \sum_{m=0}^{j-1} \theta_m' - \sum_{m=0}^{j-1} \theta_m' - \eta \sum_{m=0}^{j-1} \theta_m''$$

The computations are carried out iteratively until convergence is achieved within a tolerance of 10^{-6} . The set of linearized equations (10) - (11) The problem is solved using the Chebyshev collocation method. Since the physical domain extends over $[0, \infty]$, it is truncated to a finite interval $[0, B]$, where B is chosen sufficiently large to satisfy the far-field boundary conditions. For computational convenience, this interval is further mapped onto $[-1, 1]$ through an appropriate coordinate transformation.

$$\eta^* = (a + B) - (a - B) \frac{\xi}{2}, \quad -1 \leq \xi \leq 1 \tag{12}$$

The Gauss-Lobato collocation points, on [-1 1] are given by:

$$\xi_i = \cos\left(\frac{\pi i}{N}\right), \quad i = 0, 1, 2, 3, \dots, N \tag{13}$$

and f_i and θ_j are estimated at the above points as:

$$\left. \begin{aligned} f_i^*(\xi) &= \sum_{k=0}^N f_i^*(\xi_k) T_k(\xi_i) \\ \theta_j^*(\xi) &= \sum_{k=0}^N \theta_j^*(\xi_k) T_k(\xi_j) \end{aligned} \right\} \tag{14}$$

where $T_k(\zeta)$ is the Chebyshev polynomial at order K^{th}

Likewise, the r^{th} differentials of f_i , and θ_j are estimated as follows

$$\left. \begin{aligned} \frac{d^r f_i}{d\eta^r} &= \sum_{k=0}^N D_{ki}^{1r} f_i(\zeta_k) \\ \frac{d^r \theta_j}{d\eta^r} &= \sum_{k=0}^N D_{kj}^{1r} \theta_j(\zeta_k) \end{aligned} \right\} i = 0, 1, 2, \dots, N, j = 0, 1, 2, \dots, N \tag{15}$$

where $D^1 = \frac{2}{L} D$ with D is the Chebyshev derivatives matrix.

Using the derivative approximations in Eq. (15) within Eqs. (10)– (11) leads to the matrix form given by Eq. (16).

$$A_{j-1} X_j = R_{j-1} \tag{16}$$

where A_{j-1} represents order $2(N + 1)$ square matrix and X_j and R_{j-1} represents order $2(N + 1)$ column matrices given by

$$A_{j-1} = \begin{bmatrix} A_{11} & A_{12} \\ A_{21} & A_{22} \end{bmatrix}, \quad X_j = \begin{bmatrix} F_i \\ \theta_j \end{bmatrix}, \quad R_j = \begin{bmatrix} r_1 \\ r_2 \end{bmatrix} \tag{17}$$

Here

$$\begin{aligned} F_i &= [f_j^*(\xi_0), f_j^*(\xi_1), \dots, f_j^*(\xi), f_j^*(\xi)] *^T, \\ \theta_j &= [\theta_j^*(\xi_0), \theta_j^*(\xi_1), \dots, \theta_j^*(\xi_{n-1}), \theta_j^*(\xi)] *^T, \\ A_{11} &= a_1 D''' + a_2 D'' + a_3 I, A_{12} = 0, \\ A_{21} &= b_1^* I, A_{22} = [b_2^* D'' + b_3 D] \\ r_1 &= [r_1(\xi_1), r_1(\xi_2), r_1(\xi_3), \dots, r_1(\xi_{n+1})]^T, \\ r_2 &= [r_2(\xi_1), r_2(\xi_2), r_2(\xi_3), \dots, r_2(\xi_{n+1})]^T, \end{aligned}$$

where the $[]^T$ stands for transpose, O denotes the zero, I denote the identity matrix. By applying the boundary conditions at the selected collocation points, the solution can be obtained as

$$X_j = A_j^{-1} R_{j-1} \tag{18}$$

V. ANALYSIS AND DISCUSSION OF RESULTS

The present study computes Prandtl number Pr , the velocity(f'), temperature(θ), skinfriction coefficient (C_f) and Nusselt number (Nu), and depicted graphically.

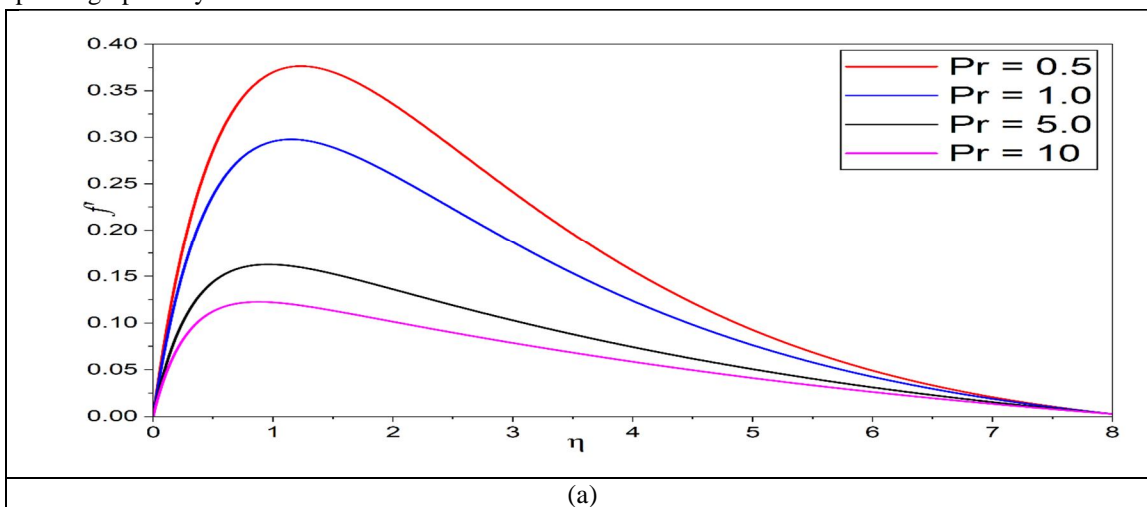


Figure 2. “Effect of Prandtl number Pr on the velocity”

As the Prandtl number Pr increases, the velocity profile f' tends to decrease, as illustrated in Figure 2(a). This decline in velocity is attributed to the fact that larger Pr values indicate reduced thermal diffusivity, which limits the rate of heat transfer within the fluid. Consequently, the thermal boundary layer becomes thinner, diminishing energy transport and slowing down fluid motion. This reduction in thermal effects also influences the momentum boundary layer, resulting in a lower velocity distribution. Overall, this trend demonstrates the strong dependence of both thermal behavior and fluid flow on the Prandtl number.

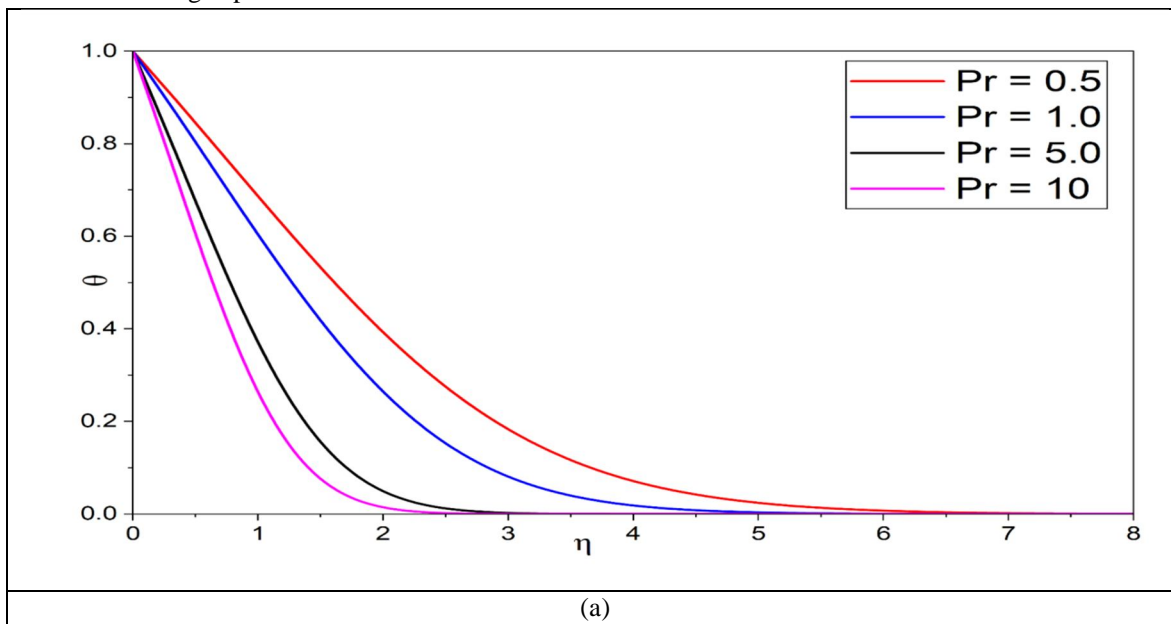


Figure 3. “Effect of Prandtl number Pr on the Temperature”

As the Prandtl number Pr rises, the temperature θ shows a decreasing trend, as observed in Figure 3(a). This effect occurs because higher Pr values correspond to lower thermal diffusivity, which limits the ability of heat to diffuse through the fluid. As a consequence, the thermal boundary layer becomes thinner, resulting in reduced temperature levels throughout the flow domain. The overall distribution of thermal energy within the fluid is therefore weakened. This behavior indicates that an increase in the Prandtl number plays a crucial role in lowering the temperature field.

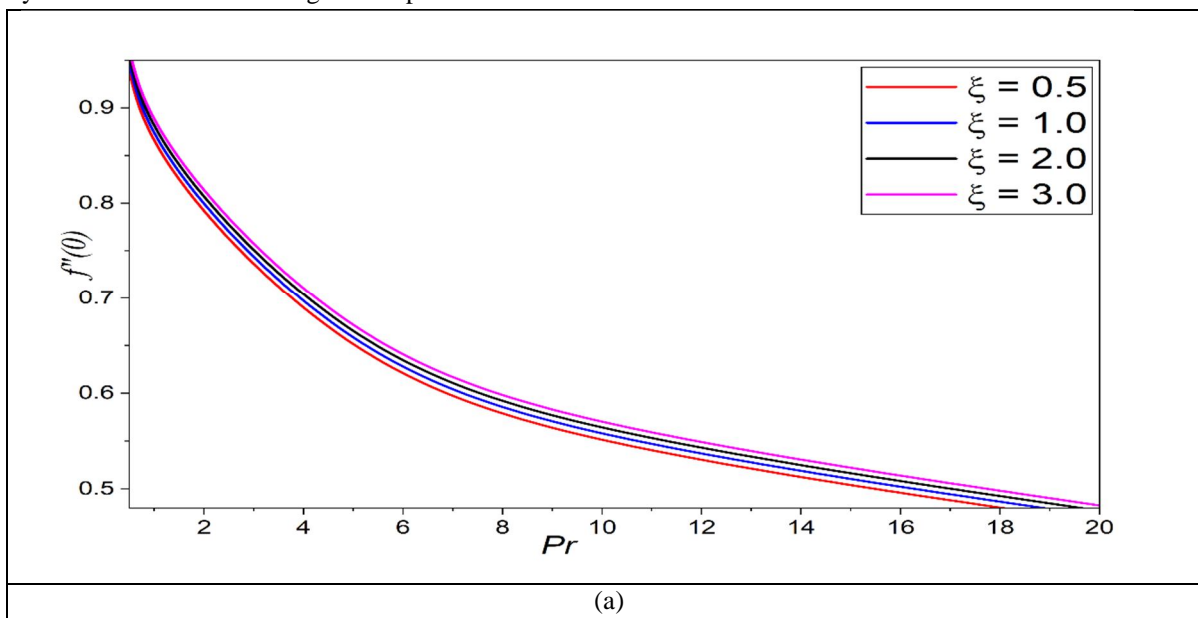


Figure 4. “Effect of skinfriction coefficient”

Figure 4(a). illustrates how the dimensionless skin friction coefficient changes with the parameter ξ It can be observed that the skin friction increases as ξ becomes larger. This trend suggests a rise in surface shear stress, likely caused by a steeper velocity gradient in the region close to the boundary layer. As ξ increases, the interaction between fluid layers and the surface becomes more significant, leading to higher resistance to flow. The upward trend observed in Figure 4(a) clearly supports this finding and demonstrates the influence of ξ on the flow characteristics.

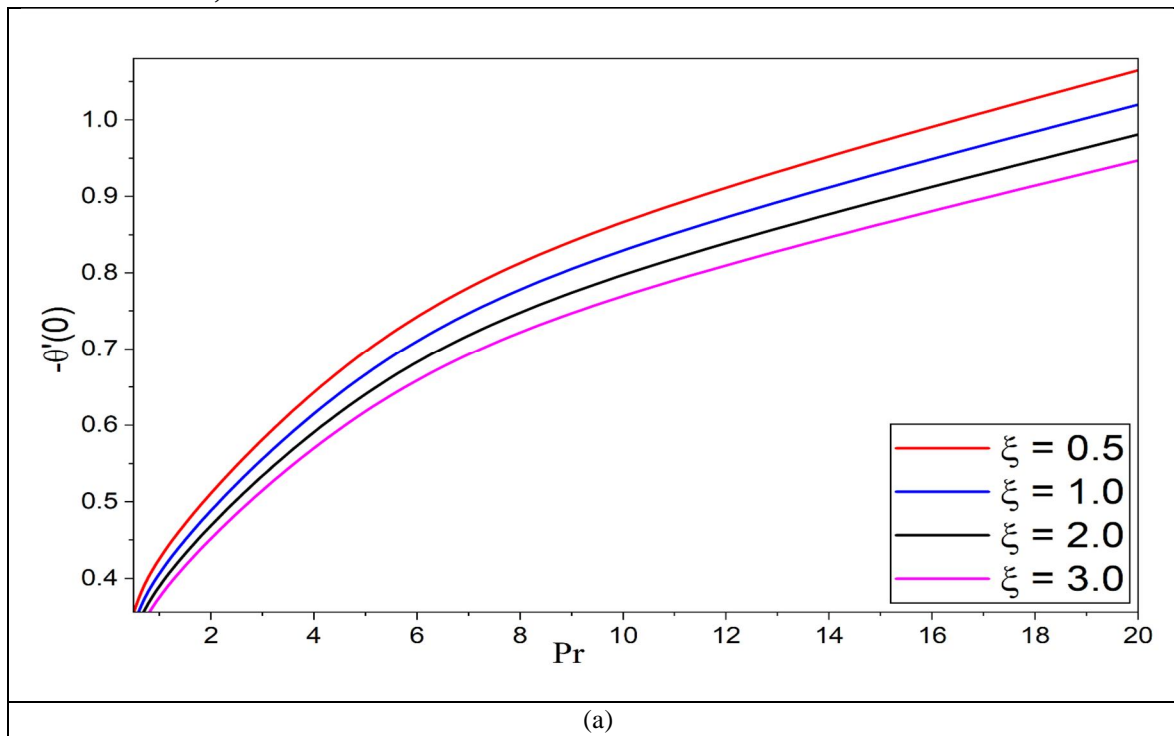


Figure 5. "Effect of Nusselt number"

Figure 5(a) presents the relationship between the Nusselt number and the parameter ξ It is evident that the Nusselt number declines as ξ increases, reflecting a decrease in heat transfer efficiency. This trend may be explained by the formation of a thicker thermal boundary layer, which hinders the transfer of heat from the surface into the surrounding fluid. As a result, the temperature gradient at the surface diminishes, leading to lower heat transfer efficiency. The downward trend shown in Figure 5(a) clearly supports this observation and highlights the influence of ξ on the thermal characteristics of the system.

VI. CONCLUSION

In conclusion, the Prandtl number Pr plays a crucial role in shaping both the temperature θ and velocity profile f' within the flow field. As Pr increases, a consistent reduction is observed in the temperature distribution due to the weakening of thermal diffusion. This results in a thinner thermal boundary layer, limiting the spread of heat across the fluid. The decline in temperature directly influences the flow behavior, since reduced thermal energy leads to weaker buoyancy forces. Consequently, the velocity profile f' also exhibits a decreasing tendency with higher values of Pr This indicates that fluids with larger Prandtl numbers tend to resist both heat transfer and fluid motion more strongly. In contrast, lower Pr values promote greater thermal diffusion, resulting in higher temperature levels and enhanced flow velocity. Overall, the interaction between thermal and momentum transport becomes more restricted as Pr rises, significantly affecting the overall dynamics of the system. Therefore, the Prandtl number serves as an important controlling parameter in determining the combined thermal and hydrodynamic behavior of the fluid. The results indicate that increasing ξ leads to a rise in dimensionless skin friction, reflecting stronger surface shear effects. This trend highlights the sensitivity of flow behavior to changes in ξ , suggesting that the parameter plays a significant role in controlling boundary layer characteristics and overall fluid resistance. The findings show that increasing ξ leads to a decline in the Nusselt number, indicating reduced heat transfer performance. This behavior reflects the impact of ξ on thermal boundary layer development, demonstrating its important role in governing temperature distribution and overall heat transfer characteristics of the system.

Conflicts of interests/Competing interests: The author declares that there are no competing interests.

REFERENCES

- [1] Khan M, Manzur M, ur Rahman M. On axisymmetric flow and heat transfer of Cross fluid over a radially stretching sheet. *Results in physics*. 2017 Jan 1;7:3767-72.
- [2] Ahmed J, Shahzad A, Begum A, Ali R, Siddiqui N. Effects of inclined Lorentz forces on boundary layer flow of Sisko fluid over a radially stretching sheet with radiative heat transfer. *Journal of the Brazilian Society of Mechanical Sciences and Engineering*. 2017 Aug;39(8):3039-50.
- [3] Sreelakshmi K, Sarojamma G, Murthy JV. Homotopy analysis of an unsteady flow heat transfer of a Jeffrey nanofluid over a radially stretching convective surface. *Journal of Nanofluids*. 2018 Feb 1;7(1):62-71.
- [4] Khan SA, Nie Y, Ali B. Multiple slip effects on magnetohydrodynamic axisymmetric buoyant nanofluid flow above a stretching sheet with radiation and chemical reaction. *Symmetry*. 2019 Sep 16;11(9):1171.
- [5] Nayak B, Mishra SR, Krishna GG. Chemical reaction effect of an axisymmetric flow over radially stretched sheet. *Propulsion and Power Research*. 2019 Mar 1;8(1):79-84.
- [6] Shahzad A, Ali R, Hussain M, Kamran M. Unsteady axisymmetric flow and heat transfer over time-dependent radially stretching sheet. *Alexandria Engineering Journal*. 2017 Mar 1;56(1):35-41.
- [7] Nadeem S, Haq RU, Akbar NS, Khan ZH. MHD three-dimensional Casson fluid flow past a porous linearly stretching sheet. *Alexandria Engineering Journal*. 2013 Dec 1;52(4):577-82.
- [8] Mahanta G, Shaw S. 3D Casson fluid flow past a porous linearly stretching sheet with convective boundary condition. *Alexandria Engineering Journal*. 2015 Sep 1;54(3):653-9.
- [9] Raju CS, Sandeep N, Sugunamma V, Babu MJ, Reddy JR. Heat and mass transfer in magnetohydrodynamic Casson fluid over an exponentially permeable stretching surface. *Engineering Science and Technology, an International Journal*. 2016 Mar 1;19(1):45-52.
- [10] Malik MY, Khan M, Salahuddin T, Khan I. Variable viscosity and MHD flow in Casson fluid with Cattaneo-Christov heat flux model: using Keller box method. *Engineering Science and Technology, an International Journal*. 2016 Dec 1;19(4):1985-92.
- [11] Nawaz M, Naz R, Awais M. Magnetohydrodynamic axisymmetric flow of Casson fluid with variable thermal conductivity and free stream. *Alexandria engineering journal*. 2018 Sep 1;57(3):2043-50.
- [12] Awais M, Raja MA, Awan SE, Shoaib M, Ali HM. Heat and mass transfer phenomenon for the dynamics of Casson fluid through porous medium over shrinking wall subject to Lorentz force and heat source/sink. *Alexandria Engineering Journal*. 2021 Feb 1;60(1):1355-63.
- [13] Sohail M, Shah Z, Tassaddiq A, Kumam P, Roy P. Entropy generation in MHD Casson fluid flow with variable heat conductance and thermal conductivity over non-linear bi-directional stretching surface. *Scientific Reports*. 2020 Jul 27;10(1):12530.
- [14] Faraz F, Imran SM, Ali B, Haider S. Thermo-diffusion and multi-slip effect on an axisymmetric Casson flow over a unsteady radially stretching sheet in the presence of chemical reaction. *Processes*. 2019 Nov 14;7(11):851.
- [15] Hayat T, Shehzad SA, Alsaedi A. Soret and Dufour effects on magnetohydrodynamic (MHD) flow of Casson fluid. *Applied Mathematics and Mechanics*. 2012 Oct;33(10):1301-12.
- [16] Kameswaran PK, Shaw S, Sibanda P. Dual solutions of Casson fluid flow over a stretching or shrinking sheet. *Sadhana*. 2014 Dec;39(6):1573-83.
- [17] Sharada K, Shankar B. MHD mixed convection flow of a Casson fluid over an exponentially stretching surface with the effects of soret, dufour, thermal radiation and chemical reaction. *World Journal of Mechanics*. 2015 Sep 29;5(9):165-77.
- [18] Oyelakin IS, Mondal S, Sibanda P. Unsteady Casson nanofluid flow over a stretching sheet with thermal radiation, convective and slip boundary conditions. *Alexandria engineering journal*. 2016 Jun 1;55(2):1025-35.
- [19] Vinod Y, Raghunatha KR, Nagappanavar SN, Nazarova N, Gupta M. Boundary layer flow of a non-Newtonian fluid over an exponentially stretching sheet with the presence of a heat source/sink. *Partial Differential Equations in Applied Mathematics*. 2025 Mar 1;13:101111.
- [20] Sarma AK, Sarma D. Unsteady magnetohydrodynamic bioconvection Casson fluid flow in presence of gyrotactic microorganisms over a vertically stretched sheet. *Numerical Heat Transfer, Part A: Applications*. 2026 Dec 31;87(1):2389338.
- [21] Kirubaharan DR, Subhashini AD, Murali G. Study of three dimensional Casson-nanofluid flow due to a linear porous stretching sheet in the presence of double diffusion effects. *Advances in Systems Science and Applications*. 2024 Nov 30;24(3):90-103.
- [22] Triveni B, Rao MV, Gangadhar K, Chamkha AJ. Heat transfer analysis of MHD Casson nanofluid flow over a nonlinear stretching sheet in the presence of nonuniform heat source. *Numerical Heat Transfer, Part A: Applications*. 2024 Jul 2;85(13):2145-64.
- [23] Min Z, Shaheen S, Arain MB, Zeeshan A, Hussein HS. AI-based analysis of heat transfer in Williamson nanofluids over a vertically stretching sheet. *International Journal of Hydrogen Energy*. 2026 Feb 11;208:153383.
- [24] Upreti H, Prakash J, Pandey AK, Tripathi D. Unsteady flow of magnetized SWCNTs-MWCNTs/H₂O over a stretching sheet with temperature-dependent properties: a comparative analysis. *Nano*. 2026 Jan 14;21(01):2550034.
- [25] Awati VB, Muchandi SS, Kumar NM, Bognár G. Heat and mass transfer in MHD-UCM nanofluid flow past a porous nonlinear stretching sheet with chemical reaction and bioconvection: a dual-method approach. *Nanotechnology Reviews*. 2026 Jan 23;15(1):20250251.



10.22214/IJRASET



45.98



IMPACT FACTOR:
7.129



IMPACT FACTOR:
7.429



INTERNATIONAL JOURNAL FOR RESEARCH

IN APPLIED SCIENCE & ENGINEERING TECHNOLOGY

Call : 08813907089  (24*7 Support on Whatsapp)